

Systems analysis of transcriptome and proteome in retinoic acid/arsenic trioxide-induced cell differentiation/apoptosis of promyelocytic leukemia

Pei-Zheng Zheng^{*†‡}, Kan-Kan Wang^{*‡}, Qun-Ye Zhang^{*‡}, Qiu-Hua Huang^{*‡§}, Yan-Zhi Du^{*¶}, Qing-Hua Zhang^{||}, Da-Kai Xiao^{*}, Shu-Hong Shen^{*}, Sandrine Imbeaud^{**}, Eric Eveno^{**}, Chun-Jun Zhao^{*}, Yu-Long Chen^{*}, Hui-Yong Fan^{*}, Samuel Waxman^{††}, Charles Auffray^{**}, Gang Jin[¶], Sai-Juan Chen^{*}, Zhu Chen^{*‡‡}, and Ji Zhang^{*¶§§}

^{*}State Key Laboratory of Medical Genomics, Ruijin Hospital, Shanghai Second Medical University, 197 Rui Jin Road II, Shanghai 200025, China; [¶]Health Science Center, Shanghai Institutes of Biological Science, Chinese Academy of Science and Shanghai Second Medical University, 225 South Chong Qing Road, Shanghai 200025, China; [†]Department of Clinical Laboratory, Union Hospital, Fujian Medical University, 29 Xinquan Road, Fuzhou, Fujian 350001, China; ^{||}National Engineering Center for Biochip at Shanghai, 151 Li Bing Road, Pudong, Shanghai 201203, China; ^{**}Genexpress, Functional Genomics and Systems Biology for Health, Laboratoire de Génétique de la Neurotransmission–Unité Mixte de Recherche 7091, Centre National de la Recherche Scientifique and Pierre and Marie Curie University of Paris 6, 94801 Villejuif, France; and ^{††}Department of Medicine, Mount Sinai School of Medicine, New York, NY 10029

Contributed by Zhu Chen, April 6, 2005

Understanding the complexity and dynamics of cancer cells in response to effective therapy requires hypothesis-driven, quantitative, and high-throughput measurement of genes and proteins at both spatial and temporal levels. This study was designed to gain insights into molecular networks underlying the clinical synergy between retinoic acid (RA) and arsenic trioxide (ATO) in acute promyelocytic leukemia (APL), which results in a high-quality disease-free survival in most patients after consolidation with conventional chemotherapy. We have applied an approach integrating cDNA microarray, 2D gel electrophoresis with MS, and methods of computational biology to study the effects on APL cell line NB4 treated with RA, ATO, and the combination of the two agents and collected in a time series. Numerous features were revealed that indicated the coordinated regulation of molecular networks from various aspects of granulocytic differentiation and apoptosis at the transcriptome and proteome levels. These features include an array of transcription factors and cofactors, activation of calcium signaling, stimulation of the IFN pathway, activation of the proteasome system, degradation of the PML–RAR α oncoprotein, restoration of the nuclear body, cell-cycle arrest, and gain of apoptotic potential. Hence, this investigation has provided not only a detailed understanding of the combined therapeutic effects of RA/ATO in APL but also a road map to approach hematopoietic malignancies at the systems level.

systems biology | self-organizing map

Acute promyelocytic leukemia (APL) is a form of acute myeloid leukemia that responds remarkably to the effect of differentiation-induction by *all-trans*-retinoic acid and the differentiation/apoptosis-inducing effect of arsenic trioxide (ATO). Cytogenetically, a translocation t(15;17)(q22;q21) is found in most APL patients, resulting in the formation of the promyelocytic leukemia–retinoic acid receptor α (PML–RAR α) fusion gene (1). The chimeric protein encoded by the fusion gene oligomerizes with retinoid-X receptor (RXR) and disrupts the retinoic acid (RA) signal pathway, which is essential for granulocytic differentiation. PML–RAR α can also form a homodimer that competes with RAR α for binding to the RA-response elements of target genes and binds to the corepressor (CoR) complex with a much higher affinity than does the wild-type RAR α /RXR. This change leads to transcriptional repression under physiological concentrations of RA and, thus, blocks cell differentiation. Pharmacological concentrations of RA can convert the PML–RAR α fusion protein from a transcription repressor to a transcription activator, resulting in the release of the CoR and the recruitment of a coactivator (CoA) complex. The RA treatment can also trigger degradation of the PML–RAR α protein via the ubiquitin/proteasome (U/P) pathway and, thus,

trigger reassembly of the nuclear body (NB) (2). On the other hand, ATO induces partial differentiation and/or apoptosis of APL cells in a dose-dependent manner. Importantly, cellular and molecular studies have shown that ATO targets PML–RAR α through inducing a rapid SUMO-1-mediated degradation of the PML moiety of fusion protein (3). More recently, a concept of synergistic targeting of the PML–RAR α oncoprotein by combining RA and ATO has been proposed, and a high-quality disease-free survival has been achieved in clinical studies (4).

Although much has been learned about interactions between RA and receptors at transcriptional regulatory sites, knowledge in terms of downstream dynamic changes leading cells to disease recovery is limited. In view of the ability of ATO to bind to a wide range of thiol-containing proteins (5), the exact mode of selective action of the compound on APL is far from clear. Understanding the clinically observed *in vivo* synergistic effects of RA and ATO represents an even greater challenge, because multilayered regulation can be implicated with the two compounds of overlapping but distinct target properties. To get insights into the complex biochemical mechanisms of this effective leukemia therapy, we conducted an investigation incorporating advanced technologies of genomics, proteomics, and computational biology throughout the process of RA, ATO, and RA/ATO-combined treatment in the APL cell line NB4, which has been well characterized for its specific response to these agents. We found numerous features with respect to molecular networks involved in various aspects of cell proliferation, differentiation, and apoptosis.

Materials and Methods

Cell Culture. Cells from NB4, a human APL cell line received from M. Lanotte (Institut National de la Santé et de la Recherche Médicale, Paris), were grown in RPMI medium 1640 supplemented with 10% FBS (GIBCO) and antibiotics in a humidified atmosphere with 5% CO₂ at 37°C. *all-trans*-RA (Sigma) was dissolved in ethanol as a stock solution at 1 mM. ATO (Sigma) was dissolved in 1 M NaOH and further diluted to 5 mM in PBS as a stock solution.

Abbreviations: APL, acute promyelocytic leukemia; ATO, arsenic trioxide; C/EBP, CCAAT/enhancer-binding protein; CPP, component-plane presentations; NB, nuclear body; PML–RAR α , promyelocytic leukemia–retinoic acid receptor α ; RA, retinoic acid; SOM, self-organizing map; U/P, ubiquitin/proteasome; TFs/CoFs, transcription factors/cofactors.

[†]P.-Z.Z., K.-K.W., Q.-Y.Z., and Q.-H.H. contributed equally to this work.

[§]To whom correspondence regarding proteome group should be addressed. E-mail: qiu-hua.huang@etang.com.

^{††}To whom correspondence regarding coordination should be addressed. E-mail: zchen@stn.sh.cn.

^{§§}To whom correspondence regarding transcriptome and bioinformatic study should be addressed. E-mail: jizhang@sibs.ac.cn.

© 2005 by The National Academy of Sciences of the USA

Cell-Sample Treatments and Differentiation/Apoptosis Assessments. NB4 cells were treated with *all-trans*-RA (0.1 μ M), ATO (0.5 μ M), and the combination of the two at the same doses as in the single-agent treatments. These concentrations were determined according to *in vitro* and *in vivo* conditions defined in ref. 6. Cell differentiation was evaluated by visualizing morphological changes with Wright's staining and CD11b antigen expression through flow-cytometry analysis, and the apoptosis was determined by annexin-V assay. For transcriptome analysis, NB4 cells were harvested at 0, 6, 12, 24, 48, and 72 h after treatment with RA, ATO, and RA plus ATO. For proteomic analysis, cells were harvested at 0, 12, and 48 h. These time courses were chosen to reflect primary or early responses of APL cells to the three drug treatments under defined concentrations (4).

Array Fabrication, Hybridization, and Real-Time RT-PCR. Microarrays with 12,630 cDNA clones representing 10,647 genes were fabricated in-house by using a Generation III spotter (Amersham Pharmacia Biosciences). cDNA clones were sequence-verified and enriched with genes expressed in hematopoietic cells (7). Untreated NB4 cells were used as the control for all experiments. Total RNA was prepared by using TRIzol (Life Technologies), further purified with an RNEasy column (Qiagen), and quantified by using an RNA LabChip kit (Agilent Technologies, Palo Alto, CA) followed by reverse-transcription labeling. Approximately 30 μ g of each RNA sample was reverse-transcribed into cDNA primed with oligo(dT) and labeled with either Cy3-dCTP or Cy5-dCTP by using Superscript II reverse transcriptase (Life Technologies). After hybridization under a standard protocol, data acquisition was performed by using a laser scanner (Axon Instruments, Union City, CA). A 2-fold change threshold was used to determine regulated genes. Quantitative real-time RT-PCR was conducted for 30 genes by using an iCycler iQ real-time PCR detection system (Bio-Rad) with SYBR green I fluorescent dye (Applied Biosystems).

Two-Dimensional Gel Electrophoresis and MS. A 2D gel system (Amersham Pharmacia Biosciences) was used for protein separation and quantification. The cell lysate of each sample, containing ≈ 250 μ g of total protein, was loaded onto isoelectric point focusing gel strips (24-cm strips with pH 4–7). The strips were rehydrated and focused to a total of ≈ 64 kV-h before second-dimensional electrophoresis. After silver staining, gels were digitized and analyzed by using a PowerLook III scanner (Maximum Technologies, Taipei, Taiwan) and IMAGEMASTER 5.0 software (Amersham Pharmacia Biosciences), respectively. All seven samples, i.e., three drug treatments with two time points each plus an untreated reference sample, were included in the same experimental batch, and a total of three independent experiments were performed. A gel-matching algorithm (IMAGEMASTER) was used to compare images between gels to find pairs of related spots, and the determination of differentially displayed/significantly changed protein spots was based on a ≥ 2 -fold change of percentage volumes. When the percentage volumes of matched spots escaped detection in one or more samples, special notes such as gray color (see Fig. 2B) were applied. In general, these spots were among the most significantly changed proteins. Differentially expressed protein spots were cut from the gels and digested with trypsin. Digested peptides were mixed with α -cyano-4-hydroxycinnamic acid and analyzed by a 4700 MALDI-TOF-TOF proteomic system (Applied Biosystems). Specific-peptide-mass fingerprints were first determined by using GPS EXPLORER V.2.0.1 (Applied Biosystems), and those undetermined proteins were further analyzed by tandem MS.

Data Mining. A software package of the self-organizing map (SOM) algorithm, implemented with the MATLAB 6.5 environment (www.cis.hut.fi/projects/somtoolbox/), was used for SOM training. Illustration of SOM outputs by bar-graph display or component-plane presentations (CPP) was conducted in the MATLAB 6.5 environment

(www.mathworks.com); 400 (20×20) neurons were used to train log-transformed (base 2) ratios of intensities between sample and control of 8,009 analyzable cDNAs over 15 samples (see Dataset 1, which is published as supporting information on the PNAS web site), and 100 neurons (10×10) were used to train log-transformed (base 2) ratios of percentage volumes between control and sample of 1,667 well separated protein spots over 6 samples.

Results and Discussion

RA-Induced Differentiation of NB4 Cells. Gene clustering of microarray data. At the transcriptome level, NB4 cells were treated with RA at a series of time points and profiled by using cDNA microarrays. Hybridization for each sample was repeated at least twice, and only data with a high correlation coefficient (≥ 0.95) were further analyzed. For data mining, we used SOM, which exerts distinct advantages in both gene clustering and its visualization (8). As shown in Fig. 1A, the SOM outputs were first visualized by bar-graph display, offering a global view of gene clustering, particularly with respect to the expression patterns of clustered genes. It can be seen that genes mapped to corner/edge areas of the map are mostly regulated, showing evidence of four major functional categories, with two down-regulated categories in the upper two corner/edge areas and two up-regulated categories in the bottom two corner/edge areas (Fig. 1A and B). A total of 1,113 genes were found modulated over RA-induced differentiation. To validate the reliability of the data, 30 randomly selected genes were analyzed by real-time RT-PCR, and the results were highly correlated with those of the array data. Representative results of 8 genes are shown in Fig. 1C. To address the clinical relevance of the results obtained in the NB4 cell line, a side-by-side comparison study was conducted through microarray, and a high correlation was revealed between NB4 cells and patient samples (data not shown).

Transcriptional remodeling and molecular pathways coordinating the RA-induced differentiation. A large number of transcription factors/cofactors (TFs/CoFs), particularly those related to hematopoiesis, were found to be up-regulated at an early stage (within 6 h) of the differentiation, clustered to the bottom-left-corner areas of the map (Fig. 1B). Among these factors are members of the CCAAT/enhancer-binding protein (C/EBP) family and the helix-loop-helix (HLH) family (Fig. 2A). Although modulations of C/EBPs, including C/EBP α , β , and ϵ in the RA-induced granulocyte differentiation have been reported (9, 10), there was a lack of coherent data in terms of the complex roles played by C/EBPs. It has been shown that dimerization of different C/EBP proteins precisely regulates the transcriptional activity of target genes (11). Accordingly, modulations of multiple C/EBPs (i.e., C/EBP β , δ , and ζ) strongly suggest that C/EBPs may undergo specific homo- and heterodimerization. Because C/EBP homologous protein (CHOP) is a dominant-negative regulator preventing heterodimer binding of C/EBP α / β to C/EBP enhancer sequences (12), CHOP's induction may represent a balanced mechanism in C/EBP action. Members of the HLH family represent another group of TFs coordinating the differentiation. Most HLH proteins have a basic amino acid motif, and these bHLH proteins behave as transactivators or repressors. However, a small number of HLH proteins lacking the basic motif, known as ID proteins, act as dominant-negative regulators of bHLH proteins (13). Although ID proteins have been previously viewed as inhibitors of cell differentiation (14), markedly increased expression of ID1 and ID2 genes in our setting strongly suggests their engagement in APL cell differentiation, probably through coordinating lineage-specific gene expression. Furthermore, other TFs/CoFs might also be involved in early-stage gene regulation, as implicated by modulation of *IRF1* (confirmed by real-time RT-PCR), *HHEX*, *SMARCD2*, and *TADA3L*. Thus, it can be deduced that global remodeling in transcription regulation occurs in APL cells upon RA treatment.

An obvious consequence of transcriptional remodeling is the modulation of genes involved in calcium signaling and effector

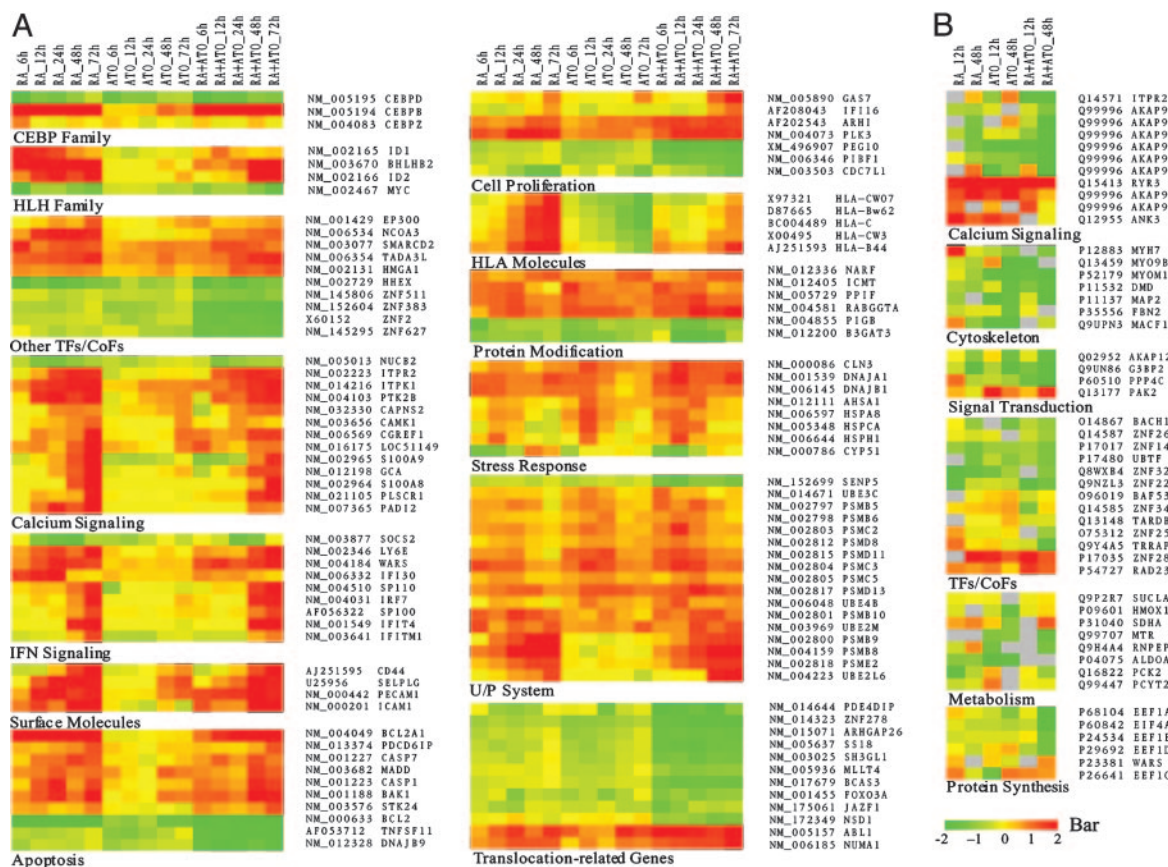


Fig. 2. Functional categories of representative genes and proteins modulated by RA, ATO, and RA/ATO in NB4 cells. (A) Genes. (B) Proteins. Ratios are color-coded as indicated by the color index bar. Gray, percentage volumes under-detected by 2D gel system. For expansion of gene/protein symbols, see *Supporting Text*, which is published as supporting information on the PNAS web site.

cells is probably triggered by different stimuli, such as overproduction of ATP inside mitochondria through activated calcium-sensitive matrix dehydrogenases.

Integration of proteomic data from RA-induced differentiation. Of the total protein spots separated by 2D gel electrophoresis, 793 appeared to be significantly changed in percentage volumes during differentiation. Of these changed protein spots, 63 were randomly chosen and further characterized by MS. Among them are TFs, signal transduction and cytoskeleton molecules, and proteins involved in calcium signaling and cell-cycle control (Figs. 1 *D* and *E* and 2*B*). The use of current technologies to establish a direct correlation between proteomic and transcriptome data is extremely challenging because of multiple layers of discrepancies, such as the distinct sensitivities of cDNA array hybridization and 2D gel electrophoresis, differences in the translational efficiency of different genes, inability of the current cDNA array platform to distinguish mRNA isoforms, posttranslational modifications of proteins that are essential for protein stability, and timing discordance of modulation at mRNA and protein levels. Proteomic data appear to be complementary to rather than duplicative of transcriptome data (see Table 1, which is published as supporting information on the PNAS web site). For example, modulation of several key members of calcium signaling was revealed only by proteome analysis, as highlighted by ryanodine receptor 3 (RYR3), an intracellular calcium-ion-release channel (Fig. 2*B*). Equally notable is AKAP9, a kinase anchor protein involved in various signal-transduction pathways, including PKA signaling (17). AKAP9 promotes the phosphorylation of inositol trisphosphate receptors through PKA and, thus, contributes to calcium regulation. The detection of at least eight spots of AKAP9 protein with distinct regulatory patterns

(Fig. 2B) provides evidence supporting the notion that AKAP9 is actively involved in multifunctional pathways probably essential for RA-induced differentiation. To this end, it may be worth pointing out that a number of cytoskeleton proteins, including calcium-sensitive/-dependent proteins, were also modulated at the proteomic level (Fig. 2B).

ATO Effects on NB4 Cells at the Transcriptome and Proteome Levels.

ATO effects at the transcriptome level. ATO-treated NB4 cells revealed a much smaller number of regulated genes (487) than did RA-treated cells (1,113), an observation that is supported by regulatory patterns of the CPP-SOM as well (Fig. 1B). This finding appears to be verified when we look further into details of the functionally classified genes. For example, a total of 74 TFs/CoFs were regulated by RA, whereas only 29 were regulated by ATO. It should be noted that many ATO-regulated genes (316 of 487, 65%) were also regulated by RA but in a more profound manner (Fig. 1B). Hence, the effects of both RA and ATO on these genes may be additive. Transcriptional modulation of many of these 316 genes could be related to essential aspects of cell-activity control, such as the induction of differentiation antigens (*PECAM1* and *SELPLG*), the modulation of apoptosis regulators (*BAK1*, *BCL2*, and *MADD*), and the regulation of genes involved in cell-cycle and growth control (*CDC7L1* and *PLK3*). Based on these observations, we assume that ATO may have some RA-like effects on APL cells, probably because of the ATO-targeted degradation of PML-RAR α . Unlike RA, ATO mainly induces the degradation rather than the activation of the hormone-inducible TF PML-RAR α . This assumption probably also explains a less-wide spectrum of regulated genes and a less-profound degree of gene regulation in cells treated by ATO

with previous data suggesting that the more degradation of the PML-RAR α occurs, the better is recovery from the disease (4). Interestingly, synergistically/additively down-regulated genes include a group of genes known to be involved in various chromosome translocations in human malignancies (Fig. 2A). For instance, *ARHGAP26*, *SH3GL1*, and *MLLT4* are translocation partners of the *MLL* gene in acute leukemia. Synergistic/additive down-regulation of these genes may represent a more effective manner of eliminating oncogenic properties or reducing cell-survival potentials in APL cells treated by RA and ATO than in those treated by RA alone or ATO alone. Moreover, a group of genes related to cell proliferation, e.g., *IFI16b* and *GAS7*, and apoptosis, e.g., *STK24*, were also found among the synergistically/additively modulated genes. On the other hand, an antagonistic effect between RA and ATO on gene regulation was also detected, although impacted genes appeared to be only a small percentage of the total. One such example is *CYP51*, a gene of the cytochrome P450 family involved in the catabolism of RA (19). *CYP51* seems to be induced by RA, whereas its induction was abolished under the joint effect of RA/ATO, possibly leading to an increased sensitivity of APL cells to RA treatment.

Proteomic features of RA/ATO-treated NB4 cells. Because RA and ATO exert preferential effects on transcriptome and proteome, respectively, it would be interesting to further investigate protein expression profiles of RA/ATO-treated APL cells. Indeed, we found that a total of 414 protein spots were synergistically/additively modified by RA/ATO on 2D gels, and some of the protein spots were characterized further, as shown in Fig. 2B. For example, translation-initiation factor EIF4A1 and translation-elongation factors EEF1B2, EEF1A1, and EEF1D were down-regulated in a much deeper way under cotreatment than those in either of the single treatments. It has been suggested that the regulation of translational factors may play a role in coordinating proliferation and tumor growth. Accordingly, synergistic/additive inhibition of these factors by RA and ATO probably favors growth arrest. Another factor belonging to this category was TRRAP, a subunit of histone acetyltransferase complexes and an essential cofactor for the c-myc and E1A/E2F-involved transcriptional regulation. RAD23B, an evolutionarily conserved factor involved in DNA-damage recognition as well as ubiquitin-mediated proteolysis (20), was one of the few synergistically/additively up-regulated proteins.

Systems View of Pathways Underlying RA/ATO Therapy of APL. Information obtained from transcriptome and proteome levels complemented by literature-mining allowed the identification of a number of pathways with temporospatial relationships, which might contribute to the mechanisms of RA/ATO-induced differentia-

tion/apoptosis of APL cells (Fig. 3). The early modulated molecules (within 6 h) are mostly TFs/CoFs associated with myeloid-specific gene expression, nuclear receptor signaling molecules, IFN pathway members, and factors involved in some other cascades. A second wave of gene/protein regulation (at 12–24 h) appears to be associated with several prominent features. First, modulation of genes/proteins seems to be an amplification of RA signaling, as highlighted by molecules involving IFN, calcium, cAMP/PKA (21), G-CSF, MAPK/JNK/p38, and TNF pathways (22). These pathways are regulated, not in an isolated situation, but in concert and harmony, thereby forming a network (Fig. 3). Second, there is a strong activation of the U/P system. Among the proteins under the control of this system is PML-RAR α . Degradation of this oncoprotein exerts a dual effect. On one hand, the transrepression caused by PML-RAR α is relieved. On the other hand, the PML released from the PML-RAR α /PML complex may lead to the restoration of the NB. Third, cell survival seems to be secured by the induction of an antiapoptotic program, which may ensure the terminal differentiation of granulocytes in RA-treated cells. After 48–72 h of treatment with RA/ATO, a third wave of gene/protein regulation with some interesting characteristics is visible. The expression of differentiation markers *SELL*, *SELPLG*, and *CD44* as well as functional molecules *DEFA3*, *DEFA4*, and *CCL2* reaches a maximum. Meanwhile, genes/proteins promoting cell cycle or enhancing cell proliferation, such as those involved in the MAPK/JNK/p38 pathway, are significantly repressed (Fig. 3). As the cells approach terminal differentiation, the expression of apoptosis agonists increases gradually. Obviously, RA exerts its effects on APL cells mainly through nuclear-receptor-mediated transcriptional regulation, whereas ATO exercises its impact through targeting multiple pathways/cascades at the levels of proteome, transcriptome, and, probably, metabolome. Although understanding the complexity and dynamics of the *in vivo* synergy between RA and ATO in APL can be more difficult than is currently recognized, this study has clearly provided a framework to reach that goal.

We thank all members of the State Key Laboratory of Medical Genomics and colleagues of the SYSTEMOSCOPE international consortium for their constructive comments and support. This work was supported, in part, by grants from the Chinese National Key Program for Basic Research (973:2004CB518606 and 973:2001CB510208), the Chinese National High Tech Program (863-2002BA711A04), the National Natural Science Foundation of China (30328028, 30300409, and 30200332), the Shanghai Commission of Science and Technology (04DZ14004), the Shanghai Rising Star Program (04QMX1427), and by the Shanghai Commission for High Education, the Samuel Waxman Cancer Research Foundation Laboratory, the Co-PI Program of Rui Jin Hospital/Shanghai Second Medical University, and the Sino-French Laboratory in Life Sciences and Genomics.

- Warrell, R. P., Jr., de The, H., Wang, Z. Y. & Degos, L. (1993) *N. Engl. J. Med.* **329**, 177–189.
- Huang, M. E., Ye, Y. C., Chen, S. R., Chai, J. R., Lu, J. X., Zhao, L., Gu, L. J. & Wang, Z. Y. (1988) *Blood* **72**, 567–572.
- Lallemant-Breitenbach, V., Zhu, J., Puvion, F., Koken, M., Honore, N., Doubekovsky, A., Duprez, E., Pandolfi, P. P., Puvion, E., Freemont, P., et al. (2001) *J. Exp. Med.* **193**, 1361–1371.
- Shen, Z. X., Shi, Z. Z., Fang, J., Gu, B. W., Li, J. M., Zhu, Y. M., Shi, J. Y., Zheng, P. Z., Yan, H., Liu, Y. F., et al. (2004) *Proc. Natl. Acad. Sci. USA* **101**, 5328–5335.
- Zhu, J., Chen, Z., Lallemant-Breitenbach, V. & de The, H. (2002) *Nat. Rev. Cancer* **2**, 705–713.
- Chen, G. Q., Shen, Z. X., Wu, F., Han, J. Y., Miao, J. M., Zhong, H. J., Li, X. S., Zhao, J. Q., Zhu, J., Fang, Z. W., et al. (1996) *Leukemia* **10**, 825–828.
- Mao, M., Fu, G., Wu, J. S., Zhang, Q. H., Zhou, J., Kan, L. X., Huang, Q. H., He, K. L., Gu, B. W., Han, Z. G., et al. (1998) *Proc. Natl. Acad. Sci. USA* **95**, 8175–8180.
- Xiao, L., Wang, K., Teng, Y. & Zhang, J. (2003) *FEBS Lett.* **538**, 117–124.
- Duprez, E., Wagner, K., Koch, H. & Tenen, D. G. (2003) *EMBO J.* **22**, 5806–5816.
- Pitha-Rowe, I., Petty, W. J., Kitareewan, S. & Dmitrovsky, E. (2003) *Leukemia* **17**, 1723–1730.
- Ramji, D. P. & Foka, P. (2002) *Biochem. J.* **365**, 561–575.
- Lekstrom-Himes, J. & Xanthopoulos, K. G. (1998) *J. Biol. Chem.* **273**, 28545–28548.
- Massari, M. E. & Murre, C. (2000) *Mol. Cell. Biol.* **20**, 429–440.
- Ying, Q. L., Nichols, J., Chambers, I. & Smith, A. (2003) *Cell* **115**, 281–292.
- Donato, R. (2001) *Int. J. Biochem. Cell Biol.* **33**, 637–668.
- Zhao, K. W., Li, X., Zhao, Q., Huang, Y., Li, D., Peng, Z. G., Shen, W. Z., Zhao, J., Zhou, Q., Chen, Z., et al. (2004) *Blood* **104**, 3731–3738.
- Tu, H., Tang, T. S., Wang, Z. & Bezprozvanny, I. (2004) *J. Biol. Chem.* **279**, 19375–19382.
- Harris, M. N., Ozpolat, B., Abdi, F., Gu, S., Legler, A., Mawuenyega, K. G., Tirado-Gomez, M., Lopez-Berstein, G. & Chen, X. (2004) *Blood* **104**, 1314–1323.
- Marill, J., Idres, N., Capron, C. C., Nguyen, E. & Chabot, G. G. (2003) *Curr. Drug Metab.* **4**, 1–10.
- Hironaka, K., Factor, V. M., Calvisi, D. F., Conner, E. A. & Thorgeirsson, S. S. (2003) *Lab. Invest.* **83**, 643–654.
- Zhao, Q., Tao, J., Zhu, Q., Jia, P. M., Dou, A. X., Li, X., Cheng, F., Waxman, S., Chen, G. Q., Chen, S. J., et al. (2004) *Leukemia* **18**, 285–292.
- Witcher, M., Ross, D. T., Rousseau, C., Deluca, L. & Miller, W. H., Jr. (2003) *Blood* **102**, 237–245.